Jpn. J. Appl. Phys. Vol. 41 (2002) pp. 1546–1556
Part 1, No. 3A, March 2002

Search for Multibody Nuclear Reactions in Metal Deuteride Induced with Ion Beam and Electrolysis Methods

Yuji ISOBE*, Shigeo UNEME, Kahou YABUTA, Yukihiro KATAYAMA, Hiroki MORI, Takayuki OMOTE, Satoshi UEDA, Kentaro OCHIAI, Hiroyuki MIYAMARU and Akito TAKAHASHI

Department of Nuclear Engineering, Osaka University, Yamadaoka 2-1, Suita, Osaka 565-0871, Japan

(Received April 27, 2001; accepted for publication November 21, 2001)

We report here the experimental results suggesting the occurrence of multibody nuclear reactions in metal deuterides under ion-beam irradiation and electrolysis. A meaningful increase of helium-4 was observed during electrolysis with the Pd–D_2O system, while neutron emission was not observed. The D + D + D fusion, $3D \rightarrow t + {}^3He + 9.5\,MeV$, has been observed repeatedly in deuteron-beam irradiation experiments with a TiD_x target. On the other hand, in proton-beam experiments with TiD_x, H + D + D-fusion: $H + D + D \rightarrow p + {}^4He + 23.8\,MeV$ was observed. Considering this result, it seems that the 3D reaction occurred between two deuterons trapped closely in TiD_x and an incident particle of deuteron. The multibody nuclear reaction model can interpret both the results obtained in electrolysis and ion-beam experiments. It is considered that the lattice dynamics of metal deuteride is of key importance for inducing short-transient and closely packed d–d pairs and, thus, such fusions. [DOI: 10.1143/JJAP.41.1546]

KEYWORDS: multibody nuclear reactions, electrolysis, helium-4, deuteron beam, proton beam, lattice dynamics

1. Introduction

Much effort has been devoted to inducing deuterium (D)-related fusion in highly D-loaded metals. Various experiments using electrolysis, beam bombardment, plasma discharge in H_2O or D_2O, discharge in D_2 gas and so forth, have been reported. Positive results have been obtained in many laboratories, *e.g.* detection of heat generation, helium-4 (^4He) production, nuclear transmutations and radiations.[1–8] Arata and Zhan have reported repeated production of a considerable amount of ^4He during electrolysis with D_2O using a specially designed Pd cathode.[9] Excess heat generation ($>10\,W$) has also been observed by them. In ion-beam experiments, emission of charged particles, which cannot be explained by a conventional nuclear reaction process in beam-target interaction, has been observed. In particular, clear evidence of an anomalous fusion by multibody nuclear reactions,[10–12] in which three or four deuterons react simultaneously, was obtained under the condition of deuteron-beam (D beam) irradiation of a titanium deuteride (TiD_x) target, as reported previously (refs. 13–15).

Various experimental approaches to induce nuclear reactions in metal deuteride have been performed in our laboratory, namely, electrolysis experiments with Pd–D_2O in a closed cell system, ion-beam experiments, experiments of plasma discharge in heavy water and stimulation experiments with metal deuteride and electron beams.[12–19] In this paper, the recent results for electrolysis and ion-beam experiments are reported. The electrolysis experiments are aimed at investigating the relationships among ^4He production, radiation (especially neutron emission) and excess heat generation. The ion-beam experiments with a D beam and TiD_x target have been performed to observe the multibody nuclear reactions. Furthermore, a new experiment with a proton beam (H beam) instead of D beam has been performed in order to investigate the dynamics required to induce the multibody nuclear reactions under D-beam irradiation. We have assumed that there is a common underlying physics between the results obtained in electrolysis and ion-beam experiments. A discussion regarding this assumption is presented in §4.

2. Electrolysis Experiment

2.1 Experimental setup and procedure

The experiment is aimed at detecting excess heat generation, neutron emission and ^4He production. Heat generation and neutron emission were measured on-line and ^4He production was examined off-line after electrolysis. The deuterium-loading ratio (D-loading ratio: D/Pd) was also measured on-line during electrolysis, since it has been argued to be an important factor in inducing nuclear reactions in solids.[20] The measurement system and electrolysis cell used in the experiments are shown in Figs. 1 and 2. Heat generation in the electrolysis cell is estimated by the mass-flow-calorimetry method. Inlet and outlet temperatures (T_{in} and T_{out}) of the coolant water were measured with two thermocouples. The flow rate of the coolant was always measured with a flow meter. From these values, heat generation in the cell was obtained. The electrolysis cell was set in a stainless-steel thermos for reducing the influence of atmospheric temperature changes. Temperatures of water in the thermostatic bath and atmosphere in and out side the stainless-steel thermos were also measured, and consistency among these values was confirmed. The decision, whether excess heat was generated or not, was made by comparing the result with that of control runs (calibration runs). In the calibration run, electrolysis was performed in the same manner and conditions, except for the cathode. A nickel (Ni) plate was used as the cathode in the calibration run since nuclear fusion has not been observed in the runs with Ni cathodes. The electrolysis cell was a closed-type cell made of stainless-steel container vessel. A coolant pipe was built in the wall and the top of the cell. Coolant water maintained at a constant temperature was made to flow through it. The cell was sealed with a metal Cu gasket and vacuumed to the level of $10^{-4}\,Pa$. The electrolyte was then introduced into this vacuous cell, and the cell was pressurized with D_2 gas. In this manner, contaminant gases could be eliminated from the cell. The inner wall of the cell was coated with a teflon

*E-mail address: yisobe@newjapan.nucl.eng.osaka-u.ac.jp

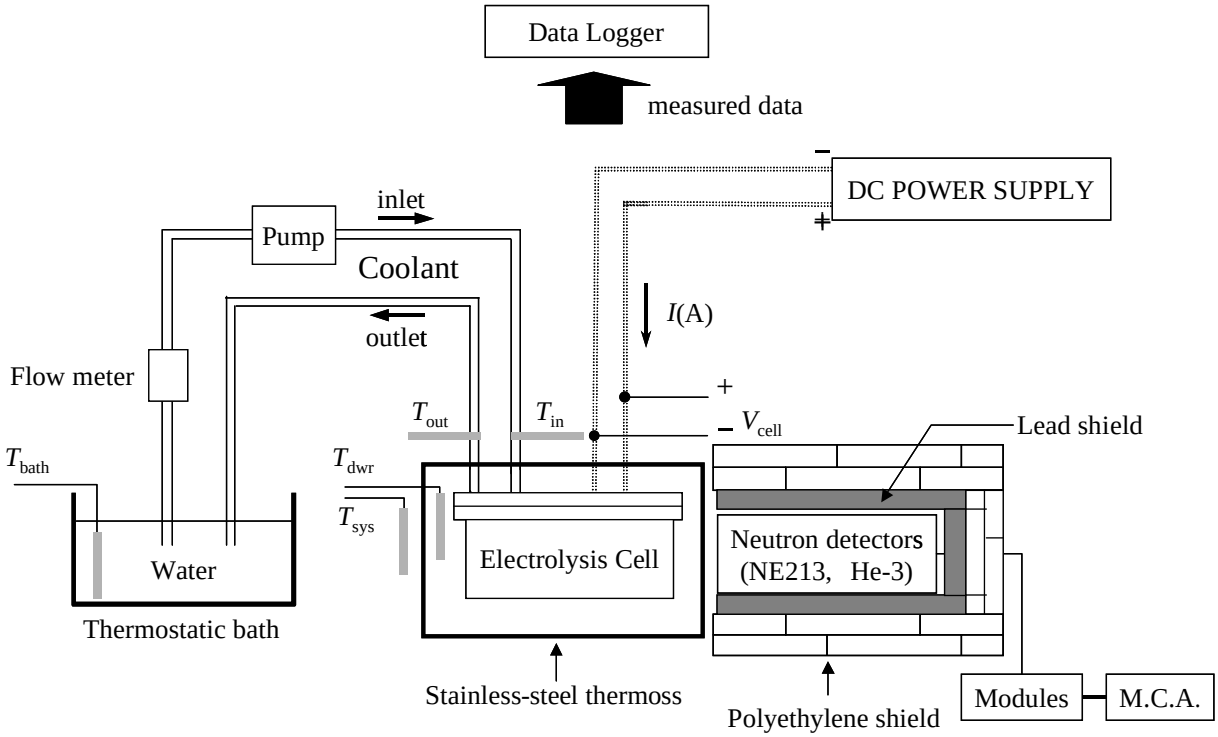

Fig. 1. Schematic view of the experimental setup.

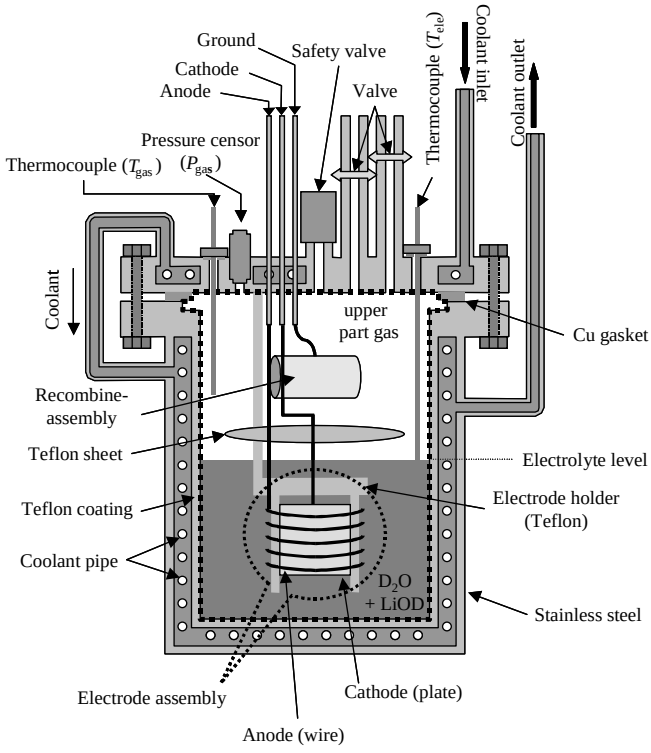

Fig. 2. Cross-sectional view of the electrolysis cell.

layer to protect the stainless-steel container from corrosion by electrolytes (alkaline solution). A recombiner assembly was set in the upper space of the cell in order to recombine generated D_2 gas and O_2 gas into D_2O. The recombiner assembly consisted of a Pt-mesh cage with a double structure. The inner cage was filled with $Al_2O_3 + Pd$ (0.5%)-alloy pellets. The outer one was filled with glass beads, which kept heavy water away from the Al_2O_3 pellets to prevent reduction of the recombination ability. The electrodes were Pd-plate cathode ($25 \times 25 \times 1\,mm^3$) and a Pt-wire anode ($1\,mm\,\phi$) respectively. Pd cathodes used in each run were treated with annealing and/or a metal-layer coating beforehand, as shown in Table I. The annealing was performed at 850°C under vacuum condition ($<10^{-5}$ Pa) for about 8 h. After the annealing, some of the cathodes were coated with a Ti or Au layer ($\sim 0.15\,\mu m$ thickness) by the vacuum evaporation method. These treatments of annealing and metal coating are expected to improve the D-loading ratio. The electrolyte consisted of D_2O ($350\,cm^2$) + LiOD (0.2 M) solution. The pattern of electrolysis operation was changed to low-high mode (the current amplitude was changed periodically between low and high current mode every 6 h: L.H.), saw-tooth mode (the current amplitude was changed like a saw tooth: S.T.), and step-up mode (the current amplitude was increased every 6 h and after several increase patterns, we decreased the current to the starting value: S.U.). D-loading ratio was calculated by measuring the pressure change of gases in the cell. A part of the D_2 gas generated at the cathode was absorbed in the cathode, while all of the O_2 gas generated at the anode was released to the upper part of the cell. This O_2 was waiting to be recombined, but the amount of D_2 gas existing as a partner of the recombination was smaller due to the absorption in the Pd cathode. The lack of the partner D_2 was filled up with previously packed D_2 gas. Consequently, the pressure of the gas in the cell decreased as the D-loading ratio in the cathode increased.

An NE213 liquid-scintillation detector (NE213) and a ^{3}He detector are employed for neutron detection. This detection system has been established for crosschecking neutron emission with two different detectors.[11] The ^{3}He detector

Table I. Experimental condition and results.

Exp. # (Duration)	D/Pd (maximum)	^{4}He detection		Neutron	Excess Heat	Pd-cathode treatment	Current mode[b)]
		Inside the cell	Inside the cathode[a)]				
1 (163 h)	0.47	No	No	No	≦1.5 W	Annealed	S.U, L.H
2 (201 h)	0.85	No	***Yes*** (**3.7×10^{14} atoms**)	No	***2.6 W*** (max.)	Annealed	S.U, L.H
3 (264 h)	0.83	No	No	No	≦1.5 W	Annealed	L.H
4 (167 h)	0.85	No	***Yes*** (**1.1×10^{15} atoms**)	No	≦1.5 W	Anneal + Ti coating	S.U, L.H
5 (243 h)	0.93	***Yes*** (**4.6×10^{16} atoms**)	***Yes*** (**8.1×10^{16} atoms**)	Not measured	≦1.5 W	Anneal + Au coating	S.U, L.H, S.T, C.C
6 (255 h)	0.96	***Yes*** (**3.3×10^{15} atoms**)	***Yes*** (**8.8×10^{14} atoms**)	Not measured	≦1.5 W	Anneal + Au coating	S.U, L.H, C.C
7 (740 h)	0.85	No	No	Not measured	≦ 1.5 W	Anneal + Au coating	S.U, L.H, S.T
8 (111 h)	0.87	***Yes*** (**2.2×10^{15} atoms**)	No	No	≦1.5 W	Anneal + Au coating	S.U, L.H

a) Analysis of gases released from electrolyzed Pd cathodes under heating up conditions.
b) S.U.: Step-up mode L.H.: Low-high mode S.T.: Saw-tooth mode C.C.: Constant-current mode.

was covered with an approximately 30-cm-thick polyethylene wall to moderate fast neutrons because the cross section of the ^{3}He(n,p)t reaction was large as the energy of neutrons distributed around the thermal energy, i.e. in order to increase the detection efficiency. The NE213 was covered with a polyethylene wall (about 30 cm thickness) and lead wall (about 5 cm thickness) except for the front facing the electrolysis cell, to reduce the influence of background neutrons. Measurements were carried out simultaneously for energy distribution (with NE213) and time variation of emission rate (with NE213 and ^{3}He detector). Measurement modules are shown in Fig. 3. Detection efficiency of each detector was 0.039% for the NE213 and 0.036% for the ^{3}He detector, respectively.

After electrolysis, gases in the upper part of the cell and the cathode were analyzed with a quadrupole mass spectrometer (QMS) in order to detect ^{4}He that was expected as an ash of presumed nuclear reactions. The cell was connected to the gas-analysis system and gas in the upper part of the cell was introduced into the analysis chamber as shown in Fig. 4. The sampling gas was sent through a sorption pump for removing most of the D_2 gas, and stored in a vacuum chamber (storage chamber). After this elimination process for obstructive elements, the resultant gas was introduced into the analysis chamber by a conductance controlled with a variable leak valve. Finally, the gas was analyzed with the QMS. The electrolyzed cathode was set on a nichrome heater in another vacuum chamber (heating chamber) after electrolysis, and the cathode was heated up to about 450°C. The released gas from the cathode was sent to the gas-analysis system and analyzed in the same manner as mentioned above. Helium-4 accumulated around the surface of Pd cathode during electrolysis could be detected by this method. The vacuum system was kept at about 10^{-7} Pa before the analysis.

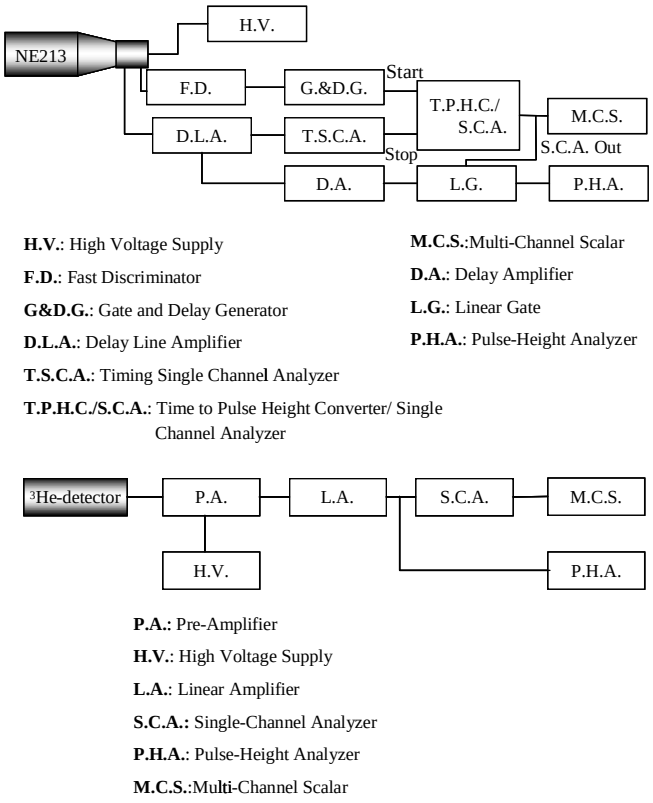

Fig. 3. Diagram of the modules for neutron measurement.

2.2 *Results and discussion*

Results and conditions of the recently performed eight runs are summarized in Table I. The positive data of ^{4}He generation were obtained in five out of eight runs. In particular, in exp. 5, a significant amount of ^{4}He was detected in the upper part gas of the cell. The probability of contamination of ^{4}He from the air was thought to be scarce, since the electrolysis cell was made of stainless steel and sealed tightly. Although the duration of the electrolysis was

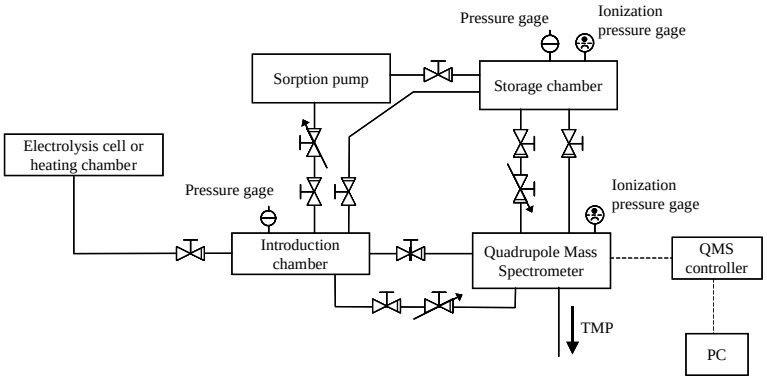

Fig. 4. Schematic view of the gas analysis system.

longer in exp. 7, such a large amount of ^{4}He was not detected. This result indicates that the amount of alien ^{4}He from the air is negligible. In exp. 5, a significant amount of ^{4}He remained in the cathode. The detected ^{4}He had to be released from the cathode, since ^{4}He was not observed before the analysis. Considering that the analysis was completed in a short time, it is difficult to explain this result as being due to the contamination of ^{4}He from the air. In exp. 6, we detected ^{4}He both in the upper-part gas and in the residual gas of the cathode. A small amount of ^{4}He was also detected in the upper-part gas in exp. 8. In exps. 2 and 4, a small amount of ^{4}He remained in the cathodes, while ^{4}He was not observed in the upper-cell gas. If this entire amount of ^{4}He (the order of 10^{15}) was produced by the DD-reaction, neutron emission at the level of 10^{12} cps should occur throughout a run. Of course, such a large amount of neutron emission should be detected by our detection system. However, no meaningful neutron emission was detected throughout this series of runs. This result indicates that the ^{4}He production is not due to the known DD-reaction but due to some other nuclear processes devoid of strong neutron emission. Excess heat generation was observed only in exp. 2. However, the level of the heat generation was low. A clear relationship between excess heat generation and ^{4}He production was not obtained. In three runs (exps. 2, 4 and 7), the same maximum values of the D-loading ratio of 0.85 were obtained. However, there is a difference among their results of ^{4}He detection. On the other hand, generation of ^{4}He was observed in every run where the maximum value of the D-loading ratio exceeded 0.85. Especially, in exps. 5 and 6, in which the D-loading ratio reached 0.9, we observed generation of ^{4}He in the Pd cathode and upper-cell gas. There is a tendency for ^{4}He generation when a high D-loading ratio ($>$0.85) is attained. Clear relationships between other parameters were not obtained in this series of runs.

3. Ion-Beam Experiments

3.1 Experimental setup and methods

The ion accelerator, OKTAVIAN at Osaka University, was used for beam bombardment experiments. Both D beam and H beam were available. The beam energy ranged from 100 keV to 300 keV and the current was about 20 μA. Ion bombardments were performed with a cylindrical vacuum chamber. A schematic diagram of the vacuum chamber and measurement system is shown in Fig. 5. Highly pre-D-loaded Ti (TiD_x; $x > 1.5$) was prepared as a target by the gas-loading method. The back of the TiD_x target was cooled with a Peltier device or coolant of gaseous liquid nitrogen (250–190 K) in order to prevent the release of D from the target under beam irradiation. Charged particles emitted from TiD_x by beam bombardment were measured with silicon-surface-barrier detectors (SSBDs). To identify charged particles, a $\Delta E\&E$-counter telescope that consisted of a thin transmission-type Si detector (ΔE detector; 26 μm thickness, effective surface area of 25 mm^2) and a conventional SSBD (E detector; depletion layer of 200 μm thickness, effective surface area of 25 mm^2) was employed. The signal from each detector was sent to a corresponding multi-channel analyzer (MCA) and the energy spectrum of each detector was thus obtained. Since linear-stopping power of Si depended on the species of charged particles, particle identification could be performed by comparing two energy spectra by the E and ΔE detectors. Another conventional SSBD (E_k detector), which had a depletion layer of 200 μm thickness and effective surface area of 25 mm^2, was set up at 120° to measure the total-energy spectrum of charged particles. A thin Al film was positioned in front of each detector in order to block scattered particles of the incident beam.

3.2 Results and discussion

Figure 6 shows energy spectra of charged particles emitted from TiD_x by D-beam (150 and 300 keV) irradiation, which were measured with the E_k detector. The detection angle was 150°. Two large count peaks of around 0.5 MeV and 2.8 MeV are those of DD-triton and DD-proton, respectively. The energy values of these peaks shift depending on the change of the beam energy. This is due to the influence of the kinematic factor of the reactions. Since kinetic energy of the DD-triton is smaller than that of the DD-proton, the effect of linear stopping power in the Al-screen foil is larger. This is the reason for the larger energy shift of DD-triton. Since count rates of these two peaks exceed 100 cps, a pile-up effect occurs for these signals for triton + triton, triton + proton and proton + proton, as shown by the broken line in Fig. 6. These pile-up factors can be estimated theoretically.[14,15] Although the shape of the spectra from 3 MeV to 6 MeV is largely affected by these pile-up factors, we can recognize the broad responses

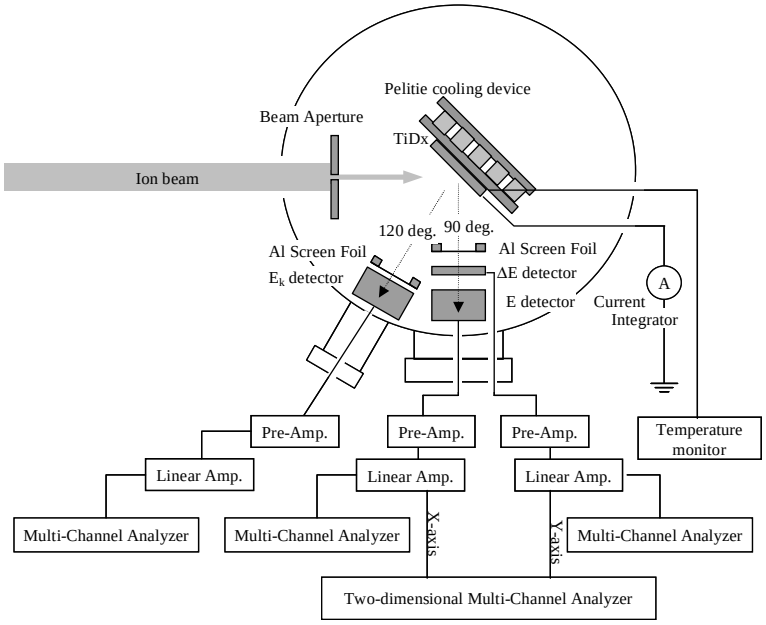

Ek-detector--effective surface area: 25mm^2, depletion layer: 200μm thickness

ΔE-detector--effective surface area: 25mm^2, 26μm thickness

E-detector--effective surface area: 25mm^2, depletion layer: 200μm thickness

Fig. 5. Schematic view of the analysis system in the ion beam experiments.

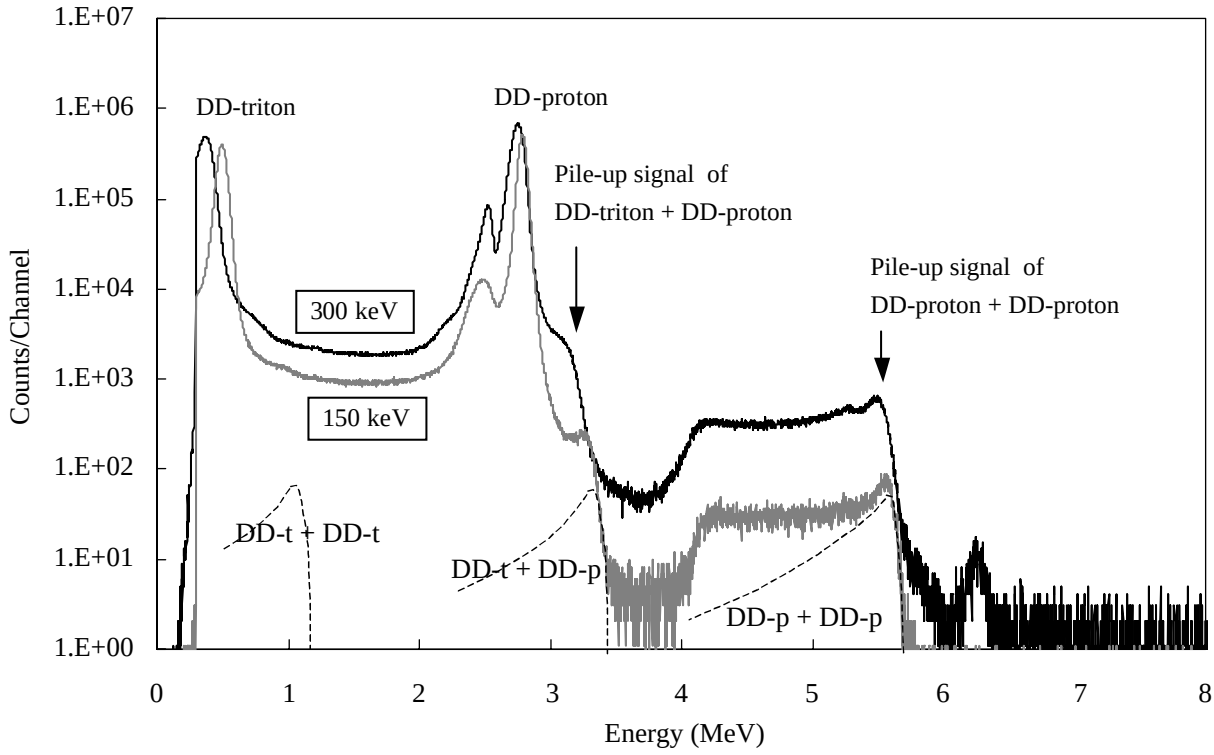

Fig. 6. Energy spectra of charged particles emitted from TiD_x under D-beam (150 keV and 300 keV) irradiation. Estimations for pile-up signals are shown with broken lines (only for 150 keV beam).

ranging from 3 MeV to 5 MeV. There is also another peak around 6.3 MeV, which can be seen only in the spectrum for the 300 keV incident beam. In order to search for these unknown responses, we show energy spectra obtained in another run by the ΔE and E detector in Figs. 7 and 8. Three spectra overlap in these figures, each of which was obtained in runs with 100, 200 and 300 keV D beams, respectively. The detection angle was 90°. Figure 7 shows the values of energy losses for each particle in the ΔE detector. Ordinarily, responses by particles of hydrogen isotopes are

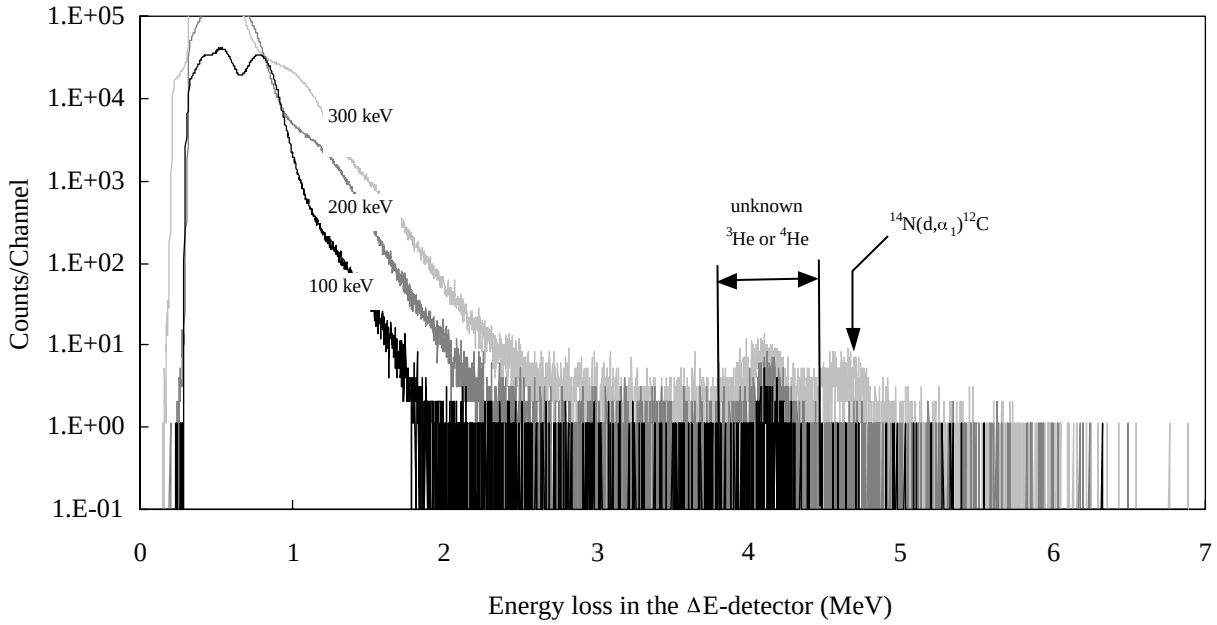

Fig. 7. Energy spectra measured with ΔE detector under D-beam irradiation of TiD_x. These energy spectra reflect the value of energy loss of emitted charged particles in the ΔE detector.

distributed below 2.5 MeV (including its pile-up) in the spectra, because of their lower linear stopping powers. The responses by DD-proton and DD-triton form two large peaks around 0.54 MeV and 0.78 MeV. The tail toward the high-energy side from these two peaks may include pile-up responses for proton + proton, proton + triton and triton + triton. We can identify two broad peaks around 4.1 MeV and 4.5 MeV. Peaks at 4.1 MeV exist for 100, 200 and 300 keV beams. The peak located at 4.5 MeV can be seen only in the spectrum of the 300 keV beam. It can be assumed that this peak was due to α-particles by the $^{14}N(d,\alpha)^{12}C$ reaction. The kinetic energy of the α-particle emitted by the $^{14}N(d,\alpha)^{12}C$ reaction is 6.4 MeV. It becomes 6.3 MeV before hitting the ΔE detector, as a result of a 0.1 MeV loss in the Al-film located in front of the detector. The α-particle with 6.3 MeV kinetic energy loses 4.3 MeV in the ΔE detector. This energy value is consistent with the observation. We should note that there is a peak around 6.3 MeV in the spectrum of the E_k detector. Therefore, this discussion indicates that the peak around 6.3 MeV in the E_k spectrum and the peak around 4.5 MeV in the ΔE spectrum are due to a common reaction such as the $^{14}N(d,\alpha)^{12}C$ reaction. The other peak at 4.1 MeV is observed in every spectrum for all beam energies, differing from the former case. This peak should also be due to the response of the ^3He or ^4He particle, considering its large energy loss value in the ΔE detector. If this energy value depends on the energy loss of the α-particle during the passage through the ΔE detector, the α-particle should have a kinetic energy of more than 6.3 MeV before hitting the ΔE detector, comparing the result obtained in the former discussion, since, ordinarily, linear stopping power becomes smaller as the kinetic energy of a charged particle becomes larger. However, we did not observe such peaks in the spectra of the E_k detector. In one more case, the peak is of ^3He with kinetic energy of about 5.3 MeV before hitting the ΔE detector. The energy loss value of 5.3 MeV-^3He is 4.1 MeV in Si of 26 μm thickness during its passage. However, we did not find any reactions that emit such ^3He among the reactions for contaminant elements. Therefore, it is reasonable to assume that the response at 4.1 MeV in the spectra of the ΔE detector is the total energy of helium-isotope particles stopping in the ΔE detector. The original energy (before hitting Al-film) of this helium-isotope particle can be calculated as 4.5 MeV for ^3He and 4.6 MeV for ^4He. First, the reaction of contaminant elements should be considered as a candidate for the source of this response. As shown in Fig. 7, this response was observed even in the experiments with a lower energy beam (100 keV). In this energy region, the Coulomb-barrier penetration probabilities of the fusion reactions for heavier elements decrease significantly. From this point of view, only light elements should be discussed as target nucleus, *e.g.*, ^6Li, ^7Li, ^9Be, ^{10}B, ^{11}B, ^{12}C, ^{13}C, ^{14}N and ^{16}O. Although reactions that emit ^3He or ^4He of about 4.5 MeV are necessary in order to explain the observed response, none of the deuteron-beam reactions with targets of ^6Li through ^{16}O have satisfied the requirement (a precise discussion about this investigation is presented in ref. 14). Therefore, other reactions should be considered. A possible channel of multibody nuclear reaction:

$$D + D + D \rightarrow t + {}^3He + 9.5\,MeV, \qquad (3.1)$$

is a highly probable candidate for explaining this response. This reaction emits ^3He with 4.75 MeV and triton with 4.75 MeV. This ^3He may lose its kinetic energy of 0.6 MeV in the layer of TiD_x and Al film set in front of the detector and enter the ΔE detector. The depth of the reaction can be calculated as 1.0 μm in TiD_x. In order to find the partner particle (4.75 MeV-triton), we need to pay attention to the spectra measured with the E detector shown in Fig. 8. There is an anomalous edge of response ranging from 3.5 MeV to 4.5 MeV, even though a double pile-up signal of DD-proton

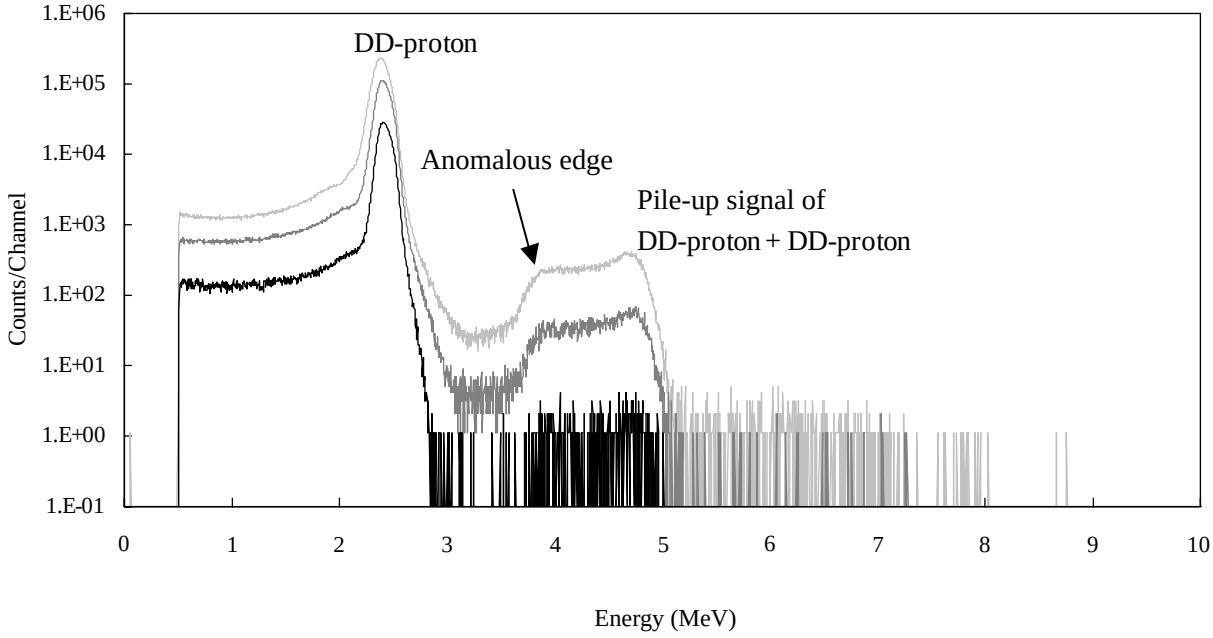

Fig. 8. Energy spectra measured with E detector under D-beam irradiation of TiD_x.

influences the shape of around there. The original kinetic energy (before Al foil) of these signals can be estimated as 4.5–5.4 MeV for triton. Assuming that α-particles with 7.5–7.9 MeV are emitted by low-energy D-beam bombardment on TiD_x, there is possibility that this response is due to α-particles. However, if this assumption is true, peaks should be observed around 3.4–3.6 MeV on the spectra of the ΔE detector, and evidently, there are no such peaks on the spectra. Moreover, no peaks are observed around 7.5–7.9 MeV on the spectra of the E_k detector. Therefore, this response may be due to particles of some hydrogen isotopes. In the reactions of contaminants, the $^9Be(d,p)^{10}B$ reaction emits 4.2 MeV protons. However, it is impossible to explain this response by the $^9Be(d,p)^{10}B$ reaction, considering its small reaction cross-section for low-energy deuteron and small contaminant density of ^9Be on TiD_x.[14,21] Consequently, the possible source of this response is restricted to the triton by reaction (3.1). Accordingly, it is conceived that we could observe evidence of the 3D-reaction generation.

As discussed in our previous paper,[14] the reaction rate of 3D-fusion (R_{3d}) vs that of DD-fusion (R_{2d}) can be estimated as $[R_{3d}/R_{2d}] \sim 10^{-30}$, assuming that the 3D-fusion takes place in a conventional nuclear process of a beam-target system as the random (cascade) nuclear reaction process. On the other hand, in this run, the total yield of each reaction was 1.5×10^2 counts for 3D-^{3}He in Fig. 7 and 1.1×10^7 counts for DD-proton in Fig. 8. We can obtain the reaction rate ratio as $[R_{3d}/R_{2d}] = 1.4 \times 10^{-5}$. This anomalous enhancement factor of the order of 10^{25} compared to the random process is similar to that of the previous works ($\sim 10^{26}$).[13–15]

Next, our interest in this reaction turns to one question: ''Does this 3D-reaction consist of three deuterons trapped in the metal?''. In order to answer this question, experiments of ion-beam irradiation to TiD_x were performed with H beam instead of D beam. If the 3D-reaction is also observed in this experiment, it can be said that the incident beam is not related to the reaction directly and only plays a role of stimulation for the lattice motion (indirect reaction). In the other case where the incident beam directly affects the nuclear reaction, we can expect to observe a three-body nuclear reaction including one proton and two deuterons (direct reaction). The following reaction is useful to confirm the occurrence of the reaction:

$$H + D + D \rightarrow p + {}^4He + Q\ (23.9\,MeV). \qquad (3.2)$$

In this reaction, proton emission of 19.1 MeV is assumed. This proton can be distinguished from other particles (*e.g.* reactions for contaminant) easily, because only this reaction can emit such high-energy protons under low-energy H-beam irradiation to TiD_x. The experimental setup was almost the same as that of the D-beam experiments. Two conventional SSBDs were set up. A thick Ni-sheet (600 μm thickness) was set before one of the SSBDs (called E_h detector). Charged particles, other than high-energy protons, cannot penetrate through this screen foil. The front face of the other detector (E_k detector) was covered with Al film of 6 μm thickness. Figure 9 shows the energy spectrum measured with the E_h detector, which was obtained under beam irradiation with a 300 keV H beam. There are several counts distributed from 1 MeV to 4 MeV. Since these counts were not detected in the other runs using other screens (both thicker and thinner) and using virgin Ti instead of TiD_x, they can be identified as charged particles. Assuming that these counts are of protons, we can estimate their original kinetic energy to be about 18.5 MeV. When using a thick metal sheet as a screen foil, the straggling significantly affects the energy distribution. Its deviation becomes $\pm$1.2 MeV in this case. However, the total count of this response was very low and the statistics were not sufficient to provide clear evidence of 19.1 MeV proton generation. Accordingly, to improve the statistics, the detector was placed close to the back of TiD_x in another run in order to increase the detection efficiency of the detector. Moreover, a film of Ti of 300 μm

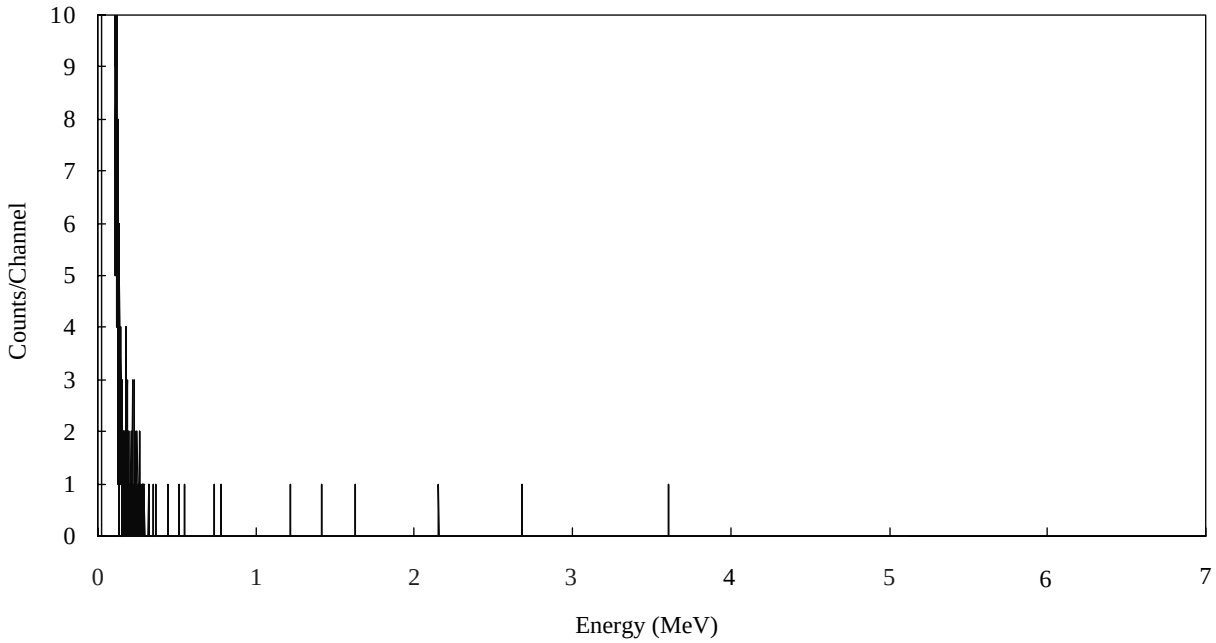

Fig. 9. Energy spectrum measured with E_h detector under H-beam irradiation of TiD_x. Front face of the E_h detector was covered with a Ni Sheet of 600 μm thickness.

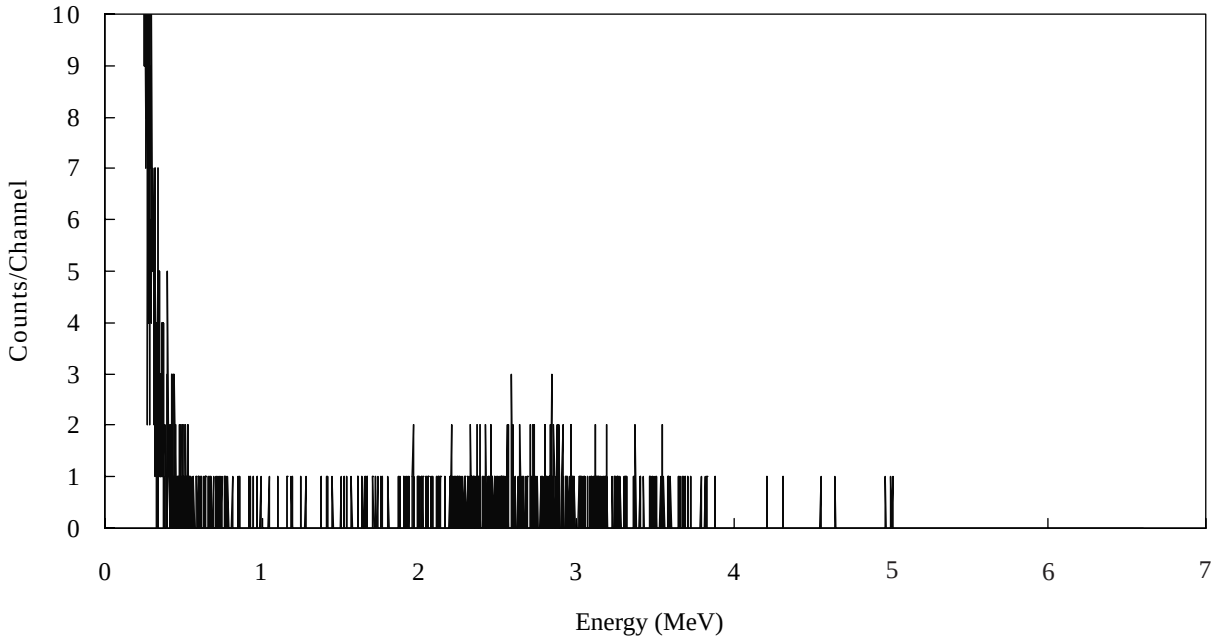

Fig. 10. Energy spectrum of high-energy charged particles measured with E_h detector under H-beam irradiation to TiD_x. E_h detector was set behind the TiD_x target. Emitted charged particles penetrate through TiD_x (1 mm) and a Ti foil (300 μm).

thickness was introduced between TiD_x and the detector since a 19 MeV-proton can penetrate through the detector (Si of 200 μm thickness) even after passing through 1 mm of TiD_x. The energy spectrum shown in Fig. 10 was obtained under this condition. A distinct broad bump is observed around 2.7 MeV. Note that the emitted charged particles have to penetrate Ti of 1300 μm thickness (1 mm of TiD_x and 300 μm of Ti-foil) to hit the detector. The original kinetic energy can be estimated to be about 19 MeV for protons. Therefore, the reaction (3.2) could be observed clearly in this condition. The partner particle of this proton (α-particle with 4.8 MeV) should be investigated. Figure 11 shows the energy spectrum measured with the E_k detector in the same run in which the energy spectrum in Fig. 9 was obtained. The responses of triton and proton by the DD-reaction are recognized at 0.6 MeV and 2.8 MeV, which are induced with deuterons knocked by an incident H beam. The peak around 3.1 MeV is due to α-particles emitted by the $^{15}N(p,\alpha)^{12}C$ reaction as contaminant.[22] A broad response ranging from 2 MeV to 4 MeV and a peak at 5.2 MeV are α-particle responses of the $^{11}B(p,\alpha_0)^8Be^*$ reaction as contaminant. It is known that the $^{11}B(p,\alpha_0)^8Be^*$ reaction emits

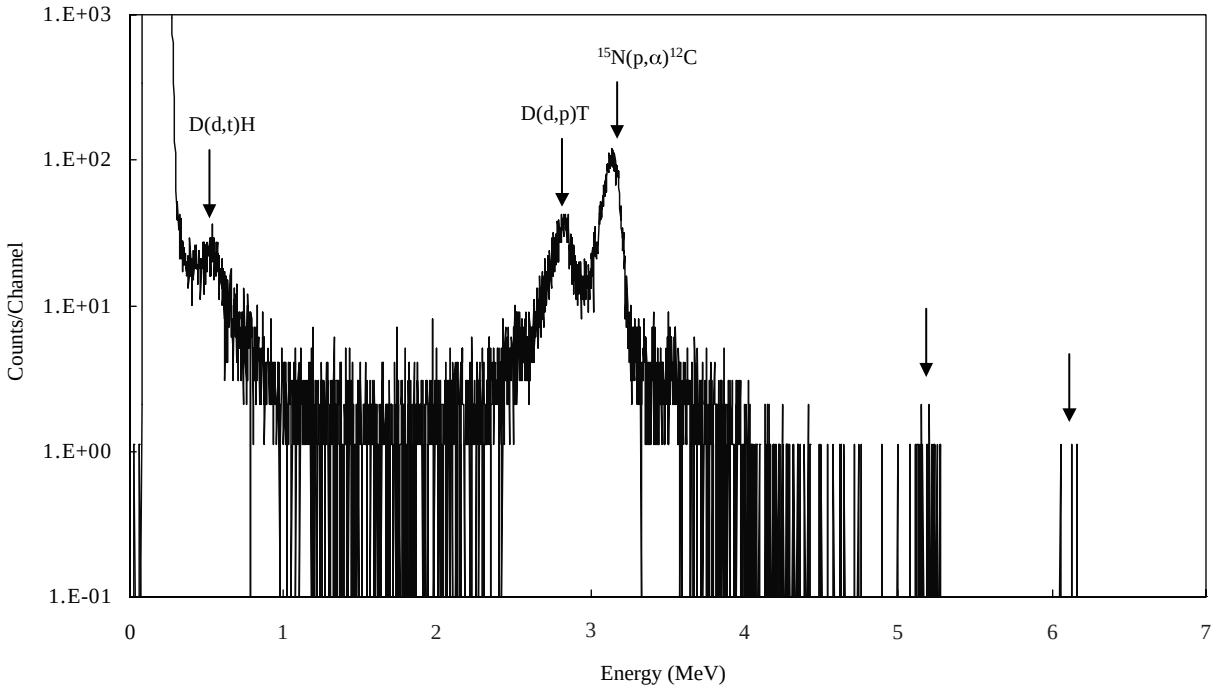

Fig. 11. Energy spectrum measured with E_k detector under H-beam irradiation of TiD_x.

three α-particles as α-particle (α_0) with 5.7 MeV and two α-particles (α_1) with continuous energy. This 5.7 MeV α-particle is expected to be located around 5.2 MeV by losing 0.5 MeV kinetic energy in Al foil. Another peak around 6.1 MeV may be a response of α-particle of the $^{19}F(p,\alpha)^{16}O$ reaction as contaminant. The partner particle of the high-energy proton (4.8 MeV α-particle) is expected to be located around 4.3 MeV, taking its energy loss in the Al film into account. In Fig. 11, unfortunately, the continuum of α-particles by the $^{11}B(p,\alpha_0)^{8}Be^*$ reaction distributes up to 4 MeV and the peak of the 4.8 MeV α-particle could not be separated. On the other hand, it is expected that 4.75 MeV triton and ^{3}He by reaction (3.1) are observed at 4.6 MeV and 4.3 MeV, if the reaction takes place in this run. However, we do not find such clear peaks in Fig. 11, although there is a possibility that the continuum overlaps on the peaks. Therefore, this result indicates that three-body nuclear fusion observed in D-beam experiments and in H-beam experiments consisted of one particle of the incident beam and two deuterons trapped in TiD_x. The reaction rate of the HDD-reaction may be less by 30 orders of magnitude than that of the DD-reaction using the same estimation performed in the case of D-beam experiments. This estimation shows that the HDD-reaction cannot be observed assuming that the reaction takes place in random processes. However, the HDD-protons could be observed (albeit several counts) in Fig. 9, even though the yield of the DD-protons detected in the same run was as low as 2.2×10^3 counts. The anomalous enhancement factor of reaction rate ratio between HDD- and DD-fusions was 10^{27} in this case.

This marked enhancement of the three-body nuclear reactions can be explained with an assumption that a high-density (in the order of 10^{10}–10^{12} pairs/cm^3) state of closely packed d–d pairs exists in TiD_x under beam irradiation condition and they are waiting for incident particles to produce three-body nuclear reactions. The inter-nucleus distance of this d–d pairs is conceived to be more than several tens of femto-meters. An appropriate distance is necessary to prevent the strong interaction between the D nuclei since significant enhancement of the DD-reaction was not observed. However, the distance should be less than 0.01 nm, i.e. within the lattice-deuteron de Broglie wavelength, in order to realize simultaneous interaction with another incident particle. The reaction rate of the 3D fusion R_{3d} can be denoted as follows, by applying the knowledge of beam-target interaction:

$$R_{3d} = N_{in} \cdot v_{in} \cdot \acute{o}_{d\text{–}dd} \cdot N_{dd}, \tag{3.3}$$

where $\acute{o}_{d\text{–}dd}$ is the cross section of the fusion reaction between incident deuterons and the closely packed d–d pair. This cross section can be approximated with a cross section of the DT-reaction, as discussed in ref. 10, namely, 4.9 b for 100 keV deuteron. The correlation among the number of the incident particles N_{in}, the velocity v_{in}, and the beam current I is given by

$$I = e{\cdot}N_{in} \cdot v_{in} \cdot S_{in}, \tag{3.4}$$

with the beam spot size area S_{in}. Using eqs. (3.3) and (3.4), R_{3d} is denoted as

$$R_{3d} = I \cdot \acute{o}_{d\text{–}dd} \cdot N_{dd} \cdot e^{-1} \cdot S_{in}^{-1}. \tag{3.5}$$

In the actual experiment, the 3D reaction ratio $R_{3d} \sim 1.4 \times 10^4$ f/(cm^3·s) was obtained under D-beam irradiation to 0.4 cm^2 beam spot size area with 100 keV beam energy and 20 μA current. The density of the closely packed d–d pair is estimated to be $N_{dd} = 9.8 \times 10^{12}$ pair/cm^3. The existence of this amount of closely packed d–d pairs in the beam spot area is necessary during the experiment. The average density of the closely packed d–d pairs N_{dd} depends on the ratio of production of the d–d pair

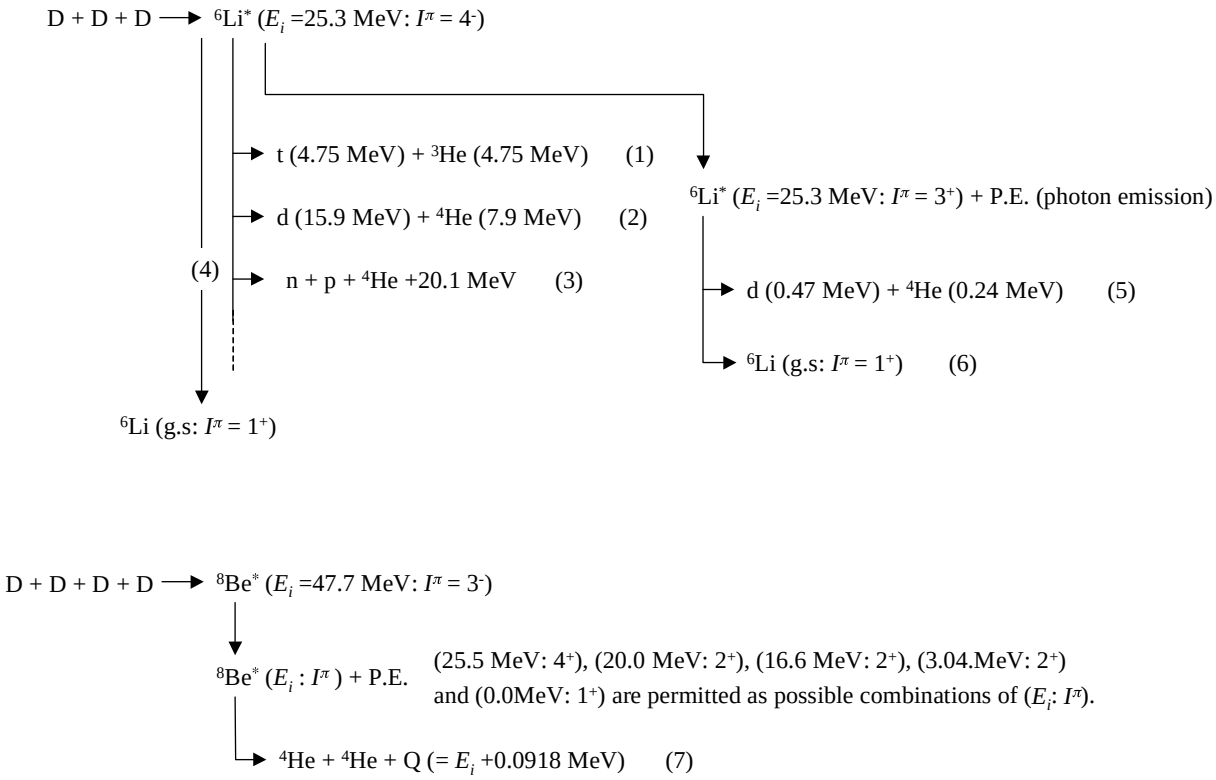

Fig. 12. Possible channels for 3D-and 4D-fusion.

R_{pair} [pair/(cm^3·s)] and its lifetime τ_{pair} (s), namely,

$$N_{\text{dd}} = R_{\text{pair}} \cdot \tau_{\text{pair}}. \tag{3.6}$$

Violante and de Ninno reported a result of a computer simulation on the mechanism for approaching d–d pairs trapped in a PdD_x lattice.[23] The result of the simulation shows that the deuteron of the d–d pair can approach each other to a distance of <0.01 nm during a very short time $\sim 10^{-17}$ s. By employing 10^{-17} s. for τ_{pair}, the order of the production ratio of the closely packed d–d pair R_{pair} can be estimated roughly as 30 orders of magnitude from eq. (3.6). This value is very large. However, we assume here that the d–d pairs in the lattice keep oscillating with a frequency and R_{pair} may depend on this frequency F_{pair}. Therefore, R_{pair} can be denoted as

$$R_{\text{pair}} = n_{\text{pair}} \cdot F_{\text{pair}}. \tag{3.7}$$

The n_{pair} is the net value of the density of the d–d pairs concerned with the production of the closely packed d–d pairs. Assuming that we can employ the ordinal plasma-oscillation frequency of metal (the order of 10^{15}–10^{16} s^{-1}) for the F_{pair}, the n_{pair} is estimated to be on the order of 10^{15}–10^{16} (pairs/cm^3) from eq. (3.7). The density of deuterium in TiD_x ($x = 1.5$) is 8.6×10^{22} D/cm^3. If all of these D atoms can form d–d pairs, 4.3×10^{22} pairs/cm^3 are possible, and then, the ratio of the n_{pair} to the total number of pairs is $1/10^6$. In this estimation, such large $\sigma_{\text{d–dd}}$ may be realized only in the case where the Coulomb repulsion is screened with many electrons. Furthermore, the mechanism for making two deuterons approach closely also needs associating electrons. We assume that deuterons rush to a reaction point or a focal point with accompanying electrons of 3d and 4s shell of Ti.

4. Discussions

In the ion-beam experiments, anomalous charged particles, which could be explained by three-body nuclear fusion (3D and HDD), were observed. Major reaction branches of multibody nuclear reactions (3D and 4D) are shown in Fig. 12, assuming three or four deuterons result in a virtual compound state of ^{6}Li* or ^{8}Be*. It is conceived that the virtual compound state of ^{6}Li* decays mainly by electromagnetic interaction (not by emissions of charged particles) since the parity of the ^{6}Li* is negative. Therefore, the outgoing channels (4), (5) and (6) may be dominant for 3D fusion. Although channel (1) has been observed in the D-beam experiments, there is possibility that the outgoing channels of (4), (5) and (6) are also present. However, the particles emitted by channel (5) do not have sufficient energy to be detected by SSBDs and energetic charged particles are not emitted by channels (4) and (6). This may be the reason that channels (4), (5) and (6) were not observed in the D-beam experiments. The meaningful increase of ^{4}He observed in electrolysis experiments can be explained on the basis of channels (5) and (7). Since the 4D fusion needs one more deuteron to react, its reaction probability seems much scarcer than that of 3D fusion. However, enhancement of the 4D reaction may be possible in a special condition, as one of the authors has proposed,[11,12] where the deuterons trapped in a metal lattice are oscillating around a focal point collectively (coherent motion) and the state of the oscillation is excited strongly. Under this condition, three or four deuterons squeeze into a focal point at a moment accompanied by many electrons and form a cluster of 3D or 4D + electrons. At this focal point, these electrons play an important role in screening the Coulomb repulsion among

nuclei. The D-related reactions 2D, 3D and 4D fusion seem to compete with each other at the focal point in this reaction process. Concerning this problem, it was predicted in refs. 11 and 12 that the rate of 2D, 3D and 4D reactions $[R_{2d}/R_{3d}/R_{4d}]$ varies as the excitation energy of deuteron oscillation in the lattice changes, i.e. the 3D or 4D reaction is dominant as the oscillation energy becomes larger. Therefore, if this strongly excited condition can be realized in the electrolysis experiments, the generation of the meaningful amount of ^{4}He could be explained. On the other hand, it is conceived that the excitation state of the oscillation was not so high in the ion-beam experiment, and as a result, many more closely packed d–d pairs were produced than the 3D or 4D cluster of trapped deuterons. However, in the other run with an ion beam, which has been described in refs. 13–15, the indirect reaction (incident deuteron did not influence the reaction directly) was observed. This result shows a possibility that the highly excited state of deuteron oscillation can be realized by stimulating metal deuteride (PdD_x or TiD_x) with an ion beam. If the ion beam only plays a role for stimulating the motion of deuterons in metal deuteride, another method (electron-beam irradiation, laser irradiation etc.) seems to play the same role. It is expected that this assumption can be confirmed by observing 3D or 4D reaction in future experiments with a proton or some other beam. It is also assumed that channels (4) and/or (6) take place during the experiments. We will be able to check this by searching for ^{6}Li generation on the electrolyzed cathode with nuclear reaction analysis (NRA) or other analysis methods.

5. Conclusion

We have observed evidence that indicates the generation of 3D fusion in the D-beam and TiD_x-system. Considering the results obtained in the experiments with H beam, the direct reaction seems to be dominant in this three-body nuclear reaction, namely, the reaction consists of two deuterons trapped in a Ti lattice and an incident particle. Estimation with the knowledge of the reaction in a random process for beam-target interaction reveals that the reaction rate of such a three-body nuclear reaction is too small to detect. Therefore, it is assumed that an unknown dynamics in a Pd–D or Ti–D system can induce this anomalous enhancement of three-body nuclear reactions. Closely packed d–d pairs expected to be produced in TiD_x as targets to be struck by incident particles. We conceive that a lattice-dynamical motion is of key importance in producing such closely packed d–d pairs. Observation of the ^{4}He production without neutron emission in the electrolysis experiments has also been reported here. These results can also be understood based on the multibody nuclear reaction model. However, the proof of a consistent relationship between the results obtained in beam experiments and in electrolysis experiments has not been found. Although we have assumed a model where the reaction rate of the multibody nuclear reactions (3D, 4D reaction) becomes larger as the energy state of the oscillation of deuteron trapped in a lattice is excited strongly, this model should be studied much more precisely with improved theoretical methods and also with further more in depth experiments. To explain both (electrolysis and ion beam) results consistently, in depth experiments with various beams, *e.g.* α-beam, electron beam, laser beams, beams with much lower energy and so forth, will be required. These methods may be effective for stimulating deuterons in TiD_x or PdD_x and inducing the lattice dynamics that we have conceived.

1) Proc. 1st Annu. Conf. Cold Fusion (University of Utah, Utah, 1990).
2) Proc. 2nd Annu. Conf. Cold Fusion (Italian Physical Society, Bologna, 1991).
3) Proc. 3rd Int. Conf. Cold Fusion (University Academy Press, Tokyo, 1993).
4) Proc. 4th Int. Conf. Cold Fusion (Trans. Fusion Technol., 1994).
5) Proc. 5th Int. Conf. Cold Fusion (Imura Europe, Monaco, 1995).
6) Proc. 6th Int. Conf. Cold Fusion (NEDO, Toya, 1996).
7) Proc. 7th Int. Conf. Cold Fusion (ENECO, Vancouver, 1998).
8) Proc. 8th Int. Conf. Cold Fusion (Italian Physical Society, Bologna, 2001).
9) Y. Arata and Y. C. Zhan: Jpn. J. Appl. Phys. **38** (1999) L774.
10) A. Takahashi: J. Nucl. Sci. Technol. **26** (1989) 558.
11) A. Takahashi, T. Iida, F. Maekawa, H. Sugimoto and S. Yoshida: Fusion Technol. **19** (1991) 380.
12) A. Takahashi, T. Iida, H. Miyamaru and M. Fukuhara: Fusion Technol. **27** (1995) 71.
13) A. Takahashi, K. Maruta, K. Ochiai and H. Miyamaru: Phys. Lett. A **255** (1999) 89.
14) K. Ochiai, K. Maruta, H. Miyamaru and A. Takahashi: Fusion Technol. **36** (1999) 315.
15) A. Takahashi, K. Maruta, K. Ochiai, H. Miyamaru and T. Iida: Fusion Technol. **34** (1998) 256.
16) A. Takahashi: Proc. 7th Int. Conf. Cold Fusion (ENECO, Vancouver, 1998) p. 378.
17) S. Ueda, K. Yasuda and A. Takahashi: Proc. 7th Int. Conf. Cold Fusion (ENECO, Vancouver, 1998) p. 398.
18) K. Ochiai, K. Maruta, H. Miyamaru and A. Takahashi: Proc. 7th Int. Conf. Cold Fusion (ENECO, Vancouver, 1998) p. 274.
19) Y. isobe, S. Uneme, K. Yabuta, H. Mori, T. Omote, S. Ueda, K. Ochiai, H. Miyamaru and A. Takahashi: Proc. 8th Int. Conf. Cold Fusion (Italian Physical Society, conf. 70, Bologna, 2001) p. 17.
20) M. McKubre, S. Crouch-Baker A. Hauser, S. Smedley and F. Tanzella: Proc. 5th Int. Conf. Cold Fusion (Imura Europe, Monaco, 1995).
21) K. Ochiai, K. Ishii, H. Miyamaru and A. Takahashi: Trans. Annu. Meet. Japan Atomic Energy Society, 1998.
22) J. R. Tesmer: *Handbook of Modern Ion Beam Materials Analysis* (Material Research Society, Pittsburgh, Pennsylvania, 1995).
23) V. Violante and A. D. Ninno: Fusion Technol. **31** (1997) 219.